ELSEVIER

Journal of Chromatography A, 969 (2002) 49–57

JOURNAL OF CHROMATOGRAPHY A

www.elsevier.com/locate/chroma

The application of molecular modelling to the interpretation of inverse gas chromatography data

I.M. Grimsey[a,*], J.C. Osborn[a], S.W. Doughty[b], P. York[a], R.C. Rowe[a,c]

[a]*Drug Delivery Group, School of Pharmacy, University of Bradford, Bradford, West Yorkshire BD7 1DP, UK*
[b]*School of Pharmaceutical Sciences, University of Nottingham, University Park, Nottingham NG7 2RD, UK*
[c]*AstraZeneca Pharmaceuticals, Alderly Park, Macclesfield, Cheshire SK10 2NA, UK*

Abstract

The use of molecular modelling in the interpretation of inverse gas chromatography data is discussed. Crystal faces can be visualised and likely cleavage planes calculated using the surface attachment energies. Assuming that the preferred cleavage plane is the crystal face with the smallest attachment energy then the predominant crystal faces of a crystalline particle can be predicted. Surface adsorption can be modelled using Van der Waals and electrostatic interactions to evaluate the interaction energies between individual atoms of the probe molecule and atoms of the test molecule orientated as in the surface. Using examples of pharmaceutical materials, modelling has been shown to be successful in the understanding of changes in the surface energetics.

Keywords: Inverse gas chromatography; Relative humidity; Surface free energy; Molecular modelling

1. Introduction

Inverse gas chromatography (IGC) has been extensively used to analyse the surface properties and the changes in surface energetics of various powders. Whilst numerical values for surface parameters are always measured and reported, it is less common to ascribe these values and changes to the precise chemical nature of the surface.

The use of molecular modelling is widespread in understanding the structure of crystals and the process of crystallisation [1,2]. From the crystal structure, the arrangement of molecules at the surface of particular crystal faces can be modelled and visualised. By investigating the calculated attachment energies of various crystal planes, slip planes in the crystal structure can be predicted [3]. In the area of drug design, modelling has been used to understand the geometric and chemical factors that influence the binding of drugs to their respective targets [4].

In recent studies of the surface energetic parameters of pharmaceutical materials [5–9], these two approaches have been applied. The molecular structure of particular powder surfaces and the geometry and interaction energies between a probe molecule and the molecules orientated as in the crystal surface have been explored. Using these techniques, the knowledge of how the surface molecules are orientated and exposed, and how a probe molecule

*Corresponding author. Tel.: +44-1274-234-754; fax: +44-1274-234-769.
E-mail address: i.m.grimsey@bradford.ac.uk (I.M. Grimsey).

0021-9673/02/$ – see front matter
PII: S0021-9673(02)00898-1

interacts, changes in the surface properties of materials, as measured by IGC, have been rationalised.

2. Experimental

2.1. Inverse gas chromatography

A sample of each powdered material was packed into a pre-silanated glass column, plugged with silanated glass wool and loaded into a standard gas chromatograph. Each column was allowed to equilibrate for at least 48 h at a temperature of 30 °C. To investigate the effect of humidity on the surface energetics, the chromatograph was adapted so that the carrier gas could be humidified in a controlled manner (after Balard et al. [10]) (Fig. 1). The carrier gas was passed through a series of gas bubbler chambers and the humidity of the carrier gas was controlled by varying the carrier gas pressure and the temperature at which the gas bubbler was held. The average relative humidity in the column was calculated using Eq. (1) as proposed by Dorris and Gray [11].

$$\%\,\mathrm{TRH} = (P^{w}_{o,sat} P_{out} / P^{w}_{o,col} P_{sat}\, j) \times 100 \quad (1)$$

where $P^{w}_{o,sat}$ is the vapour pressure of water at the temperature of the gas bubbler, P_{out} is the pressure at the column outlet, $P^{w}_{o,col}$ is the vapour pressure of water at the temperature of the column, P_{sat} is the pressure of the gas bubbler and j is the gas compressibility factor [12].

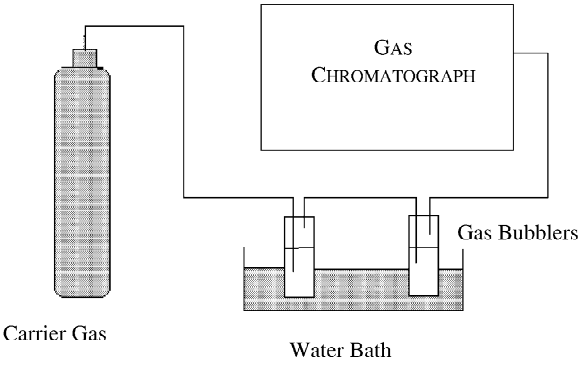

Fig. 1. The chromatography unit modified to humidify the carrier gas.

The retention times (t_r) of a series of *n*-alkanes (non-polar probes) and polar probes were measured and converted to the retention volume (V_N) using:

$$V_N = (t_r - t_d) F\, j \quad (2)$$

where F is the carrier flow-rate and t_d the retention time of a non-interacting marker.

Each probe was injected three times and the average retention time taken. The method of Schultz et al. [13] was used to determine the dispersive component of the surface-free energy (γ^{D}_{S}) using a series of *n*-alkanes (Fig. 2).

$$RT \ln V_N = a(\gamma^{D}_{L})^{1/2}\, 2N(\gamma^{D}_{S})^{1/2} + C \quad (3)$$

where N is Avogradro's number, a is the probe interaction surface area and R is the gas constant.

The specific component of the free energy of adsorption) is calculated by plotting the retention volumes (V_N) of the polar probes on the same set of axes. These data points will lie above the line formed by the alkane probes and $-\Delta G^{SP}_{A}$ is given by the deviation of each point from the alkane line (Fig. 2).

2.2. Modelling of the crystal structure and surface

The structure and surface of each material was modelled in a similar way. The single crystal structure was obtained either from the literature or from the Cambridge Structural Database (Cambridge Crystallographic Data Centre, Cambridge, UK). If

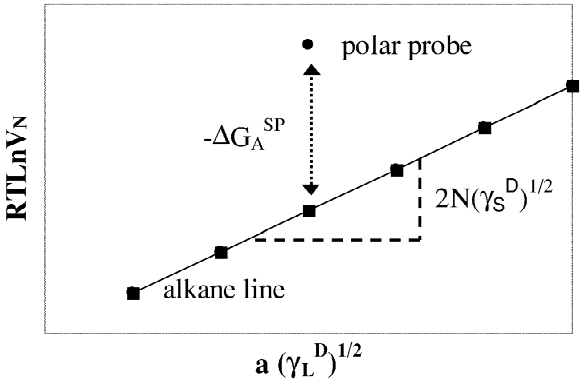

Fig. 2. Schematic diagram showing the determination of the dispersive and specific components of the standard free energy of adsorption.

necessary, the hydrogen atom positions in the structures were adjusted to compensate for the imprecision of hydrogen location by X-ray diffraction. The electrostatic potential around the isolated molecule was determined by ab initio molecular orbitals calculations at the Hartree–Fock 6-31G** level using the GAMESS (General Atomic and Molecular Electronic Structure System) molecular orbitals package [14]. Point charges were assigned to each atom using the CHELPG least-squares fitting scheme [15] to duplicate the electrostatic potential distribution around each molecule. Hydrogen bonds and Van der Waals type interactions were modelled using potentials taken from the DREIDING generic force field [16]. The van der Waals potentials are of the Buckingham (exponential-6) form while the hydrogen bond potential is an angle-dependent function. The electrostatic, van der Waals and hydrogen bond potentials were used to calculate surface attachment energies with either the MARVIN surface modelling program [17] (DL-propranolol hydrochloride) or Cerius^2 (version 3.7) (Molecular Simulations, San Diego, CA, USA) (paracetamol, carbamazepine and tolbutamide). The cleavage planes were then predicted using the assumption that the most probable cleavage plane is that having the smallest attachment energy [3]. Cerius^2 was also used to visualise the molecular arrangement in the crystal surfaces.

2.3. Calculation of probe–molecule interaction

Molecular coordinates were obtained as described in the previous section. The Van der Waals and electrostatic interactions between this molecule representing the crystal surface and a probe molecule, was calculated using the program GRID (Version 16, Molecular Discovery, Oxford, UK) [4] by evaluating the interaction energies throughout and around the test molecule. Water molecules are treated as an electrically neutral sphere with no dipole moment but capable of donating or accepting up to two hydrogen bonds. The acetone probe was modelled using a carbonyl oxygen and the tetrahydrofuran (THF) probe by considering the oxygen atom of the furan ring. Contours of equal energy are then plotted around the test molecule with negative interaction energies denoting regions of favourable interaction. The preferential interaction sites for each probe can then be predicted from the position and orientation of these regions.

3. Results and discussion

3.1. Effect of milling on the surface properties of DL-propranolol hydrochloride [5] and paracetamol [6]

Both DL-propranolol hydrochloride and paracetamol (Table 1) demonstrated similar trends in their surface energy as the particle size was reduced. In both cases the dispersive component (γ_S^D) and the specific component (ΔG_A^{SP}) for an acidic probe (chloroform or dichloromethane) increased, whilst the specific component for a basic probe (THF) decreased. This implies that the overall surface is showing an increase in both its apolar and basic

Table 1
Surface energetic parameters for milled DL-propranolol hydrochloride and paracetamol

Sample	Particle size (μm)	γ_S^D (mJ m^{-2})	ΔG_A^{SP}		
			Chloroform (kJ mol^{-1})	Dichloromethane (kJ mol^{-1})	THF (kJ mol^{-1})
Paracetamol	38.9	51	0.33		7.1
	11.3	59	0.42		6.3
	10.4	58	0.43		6.2
DL-Propranolol hydrochloride	74.7	46		2.6	2.1
	21.2	56		2.9	1.5
	14.1	61		3.0	1.2
	8.3	61		3.1	1.4
	6.6	57		2.9	1.3

properties, with a corresponding decrease in its acidic component.

As the material is being size reduced, it is assumed that the particles will preferentially split along the preferred cleavage plane, which has been assumed to be the crystal face with the smallest attachment energy [3]. The surface structure of the preferred cleavage plane in each of these materials ($(10\bar{1})$ for DL-propranolol hydrochloride and (010) for paracetamol) are shown in Fig. 3. In the case of

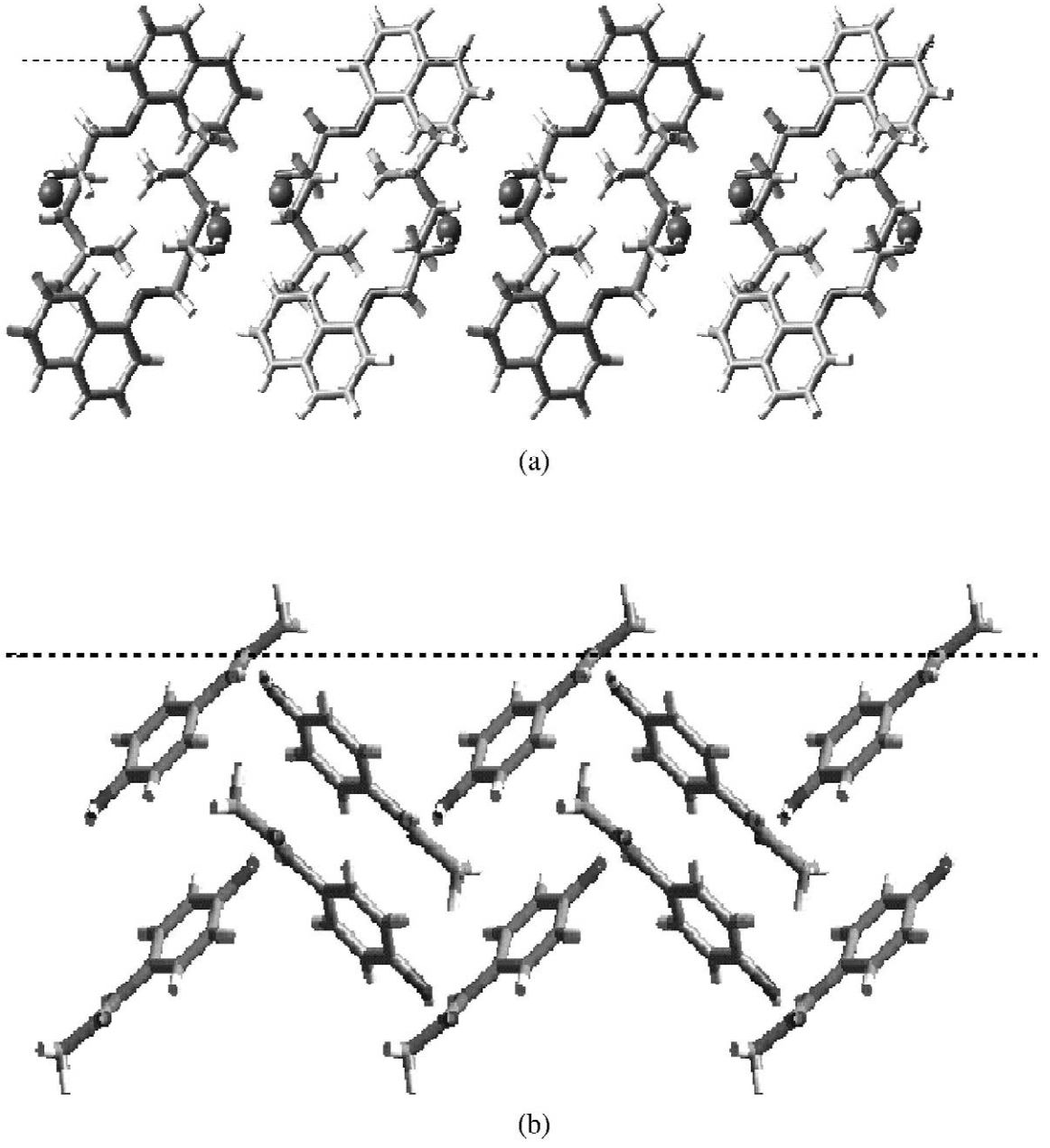

Fig. 3. The preferred cleavage plane for (a) DL-propranolol hydrochloride and (b) paracetamol.

DL-propranolol hydrochloride, the $(10\bar{1})$ face is dominated by naphthalene rings whose delocalised electrons are weak electron acceptors, strong electron donors and are more easily polarised. For paracetamol, the (010) plane (Fig. 3) reveals the preferential exposure of the hydrophobic methyl group and 'pockets' containing benzene ring moieties together with the carbonyl functionality. The phenolic OH moiety appears sterically hindered and inaccessible to any adsorbing probes. Both these faces demonstrate a chemistry which would therefore cause an increase in the overall apolar and basic nature of the material, coupled with a corresponding decrease in the acidic nature. Consequently the observed changes in the surface energetic data as measured by IGC can be correlated with the increase in the dominance of the crystal face which has the smallest attachment energy and will be preferentially exposed upon milling.

3.2. The effect of relative humidity on the surface energetics of carbamazepine and paracetamol [8] and tolbutamide [9]

Using the modified gas chromatograph (Fig. 1), the surface energetic properties of carbamazepine, paracetamol and tolbutamide were analysed at 0% RH ('dry') and 45–47% RH ('ambient') (Table 2). For paracetamol, no changes were observed in the dispersive component of the surface-free energy (γ_S^D). The values for the specific interactions with acetone and THF (ΔG_a^{SP}) were seen to decrease. For carbamazepine no changes were observed in the dispersive component of the surface-free energy (γ_S^D) or the specific components of the free energy of adsorption (ΔG_A^{SP}). For tolbutamide, again no significant change was measured in the value of γ_S^D but significant increases were seen in the values of ΔG_a^{SP} for acetone and THF.

Balard et al. [10] proposed that the decrease in surface energetic parameters, in the presence of water, was due to the water shielding the interaction sites from the vapour probes. To test this hypothesis, the interactions sites for each probe (including water) around the molecules of the powdered solid (as orientated in the surface) were predicted (Figs. 4–6) and the areas of preferential interaction plotted. The preferential sites for acetone were, in all cases, very similar to those predicted for THF.

For carbamazepine, water was found to cluster around the side chain whilst the alkyl and THF probes were found to have stronger interactions along the line of the ring structure. In Fig. 4, it can be clearly seen that the preferential interaction regions for water and the other probes do not overlap. In the case of paracetamol, the predicted interaction regions for water were around the terminal hydroxyl group and the amine and carbonyl chain. THF shows similar interaction areas around the hydroxyl and amine groups whilst the modelling shows the alkyl probes interacting most strongly in a direction perpendicular to the aromatic ring. The similarity of the interaction regions between water and THF and the disparity of the interaction regions for water and the alkyl probe are shown in Fig. 5. By a comparison of the predicted preferential interaction sites for each probe and water it was found that in the cases where there was no change in the surface energetics with relative humidity (all probes for carbamazepine and the alkanes (γ_S^D) for paracetamol) the preferential interaction regions did not show any similarity. In the cases where a decrease was

Table 2
The measured surface energetic parameters, and the standard deviations for repeat injections, for the pharmaceutical powders measured under dry and ambient conditions

Material	Calculated RH (%)	γ_S^D (mJ m^{-2}) (SD)	$-\Delta G_A^{SP}$ (kJ mol^{-1}) (SD)	
			Acetone	THF
Paracetamol	0	58.7 (1.8)	7.48 (0.07)	6.05 (0.08)
	47	60.8 (1.1)	7.12 (0.09)	5.42 (0.07)
Carbamazepine	0	57.8 (0.9)	3.59 (0.04)	1.28 (0.02)
	47	57.3 (0.7)	3.55 (0.07)	1.31 (0.02)
Tolbutamide	0	34.09 (0.83)	4.21 (0.03)	2.92 (0.04)
	45	31.93 (1.47)	4.82 (0.14)	3.59 (0.10)

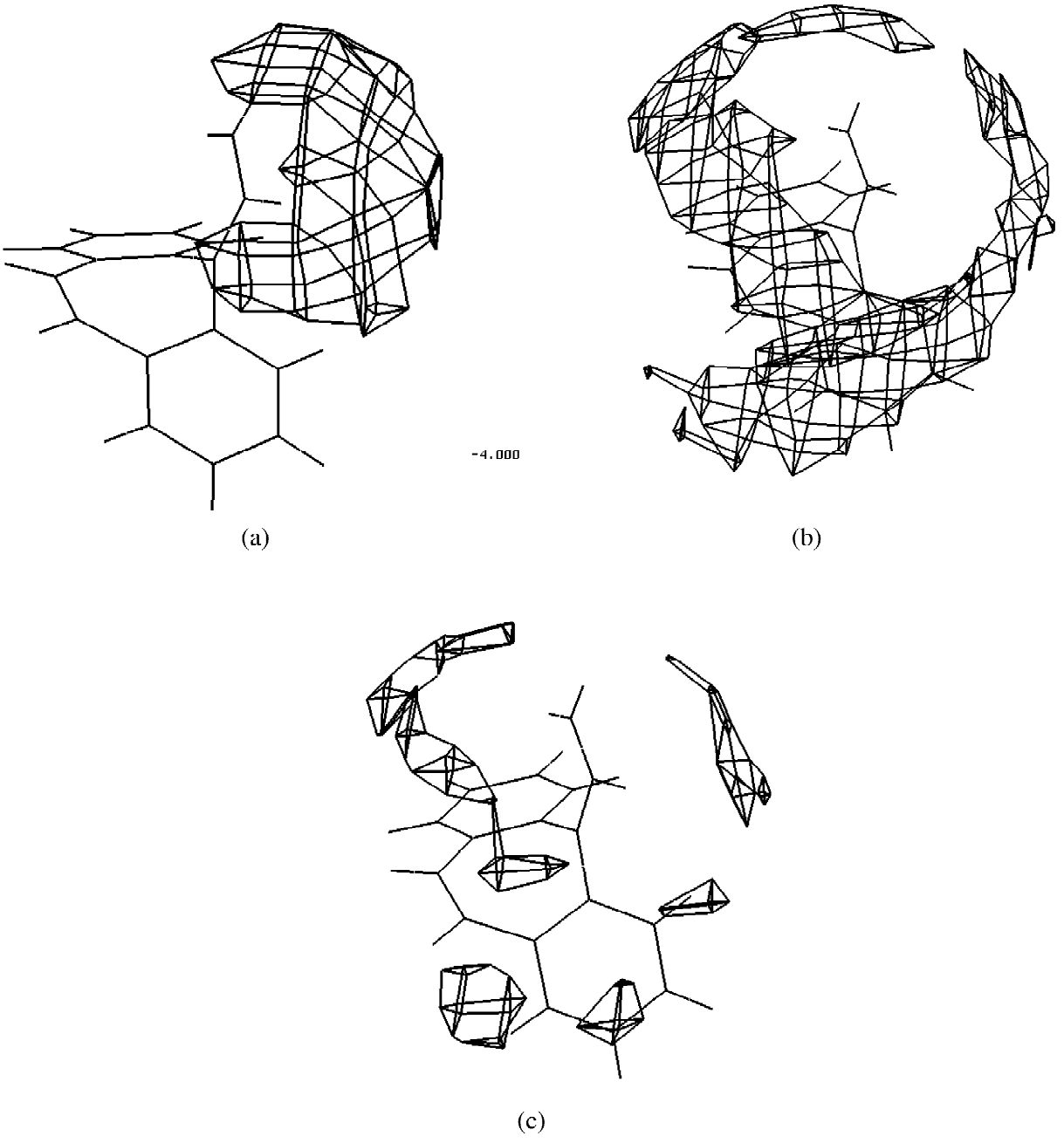

Fig. 4. The predicted preferential interaction sites of (a) water, (b) alkanes and (c) THF around carbamazepine.

observed (acetone and THF for paracetamol), the interaction regions were equivalent which supports the blocking mechanism proposed by Balard et al.

The changes in the surface energetic parameters for tolbutamide went contrary to expectation and the strength of the interactions with the polar probes (ΔG_A^{SP}) increased as the humidity increased. From the modelling of the probe interactions (Fig. 6) the

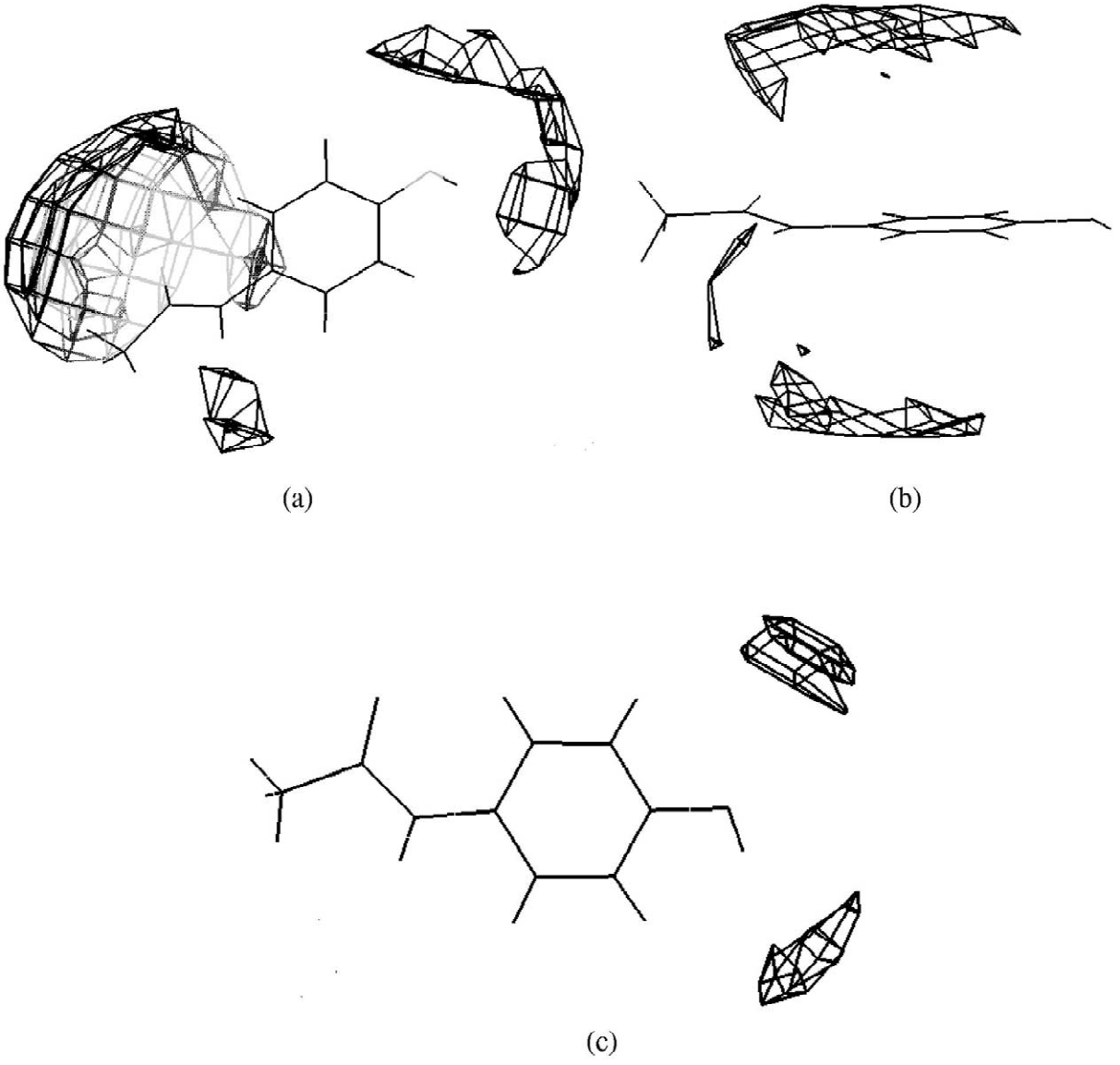

Fig. 5. The predicted preferential interaction sites of (a) water, (b) alkanes and (c) THF around paracetamol.

preferential site of interaction for the alkyl probes was centred around the ring with weaker interactions along the alkyl chain. For water, the primary site of interaction was found to be one of the NH hydrogen atoms and the carbonyl oxygen atom, with weaker interactions along the chain of the molecule. Whilst there are similarities in the interaction areas between the alkyl and water probes, the strongest sites of interaction are distinctly different and it can be proposed that the surface energetic parameters are primarily controlled by the highest energy, preferential interaction sites. The preferential interaction sites predicted for THF and acetone were around both NH groups, in contrast to the water probe that targeted only one of these groups. In this case the presence of water increased the interaction of the polar probe with the molecule even though the water is blocking one of the interaction sites. This appears to run

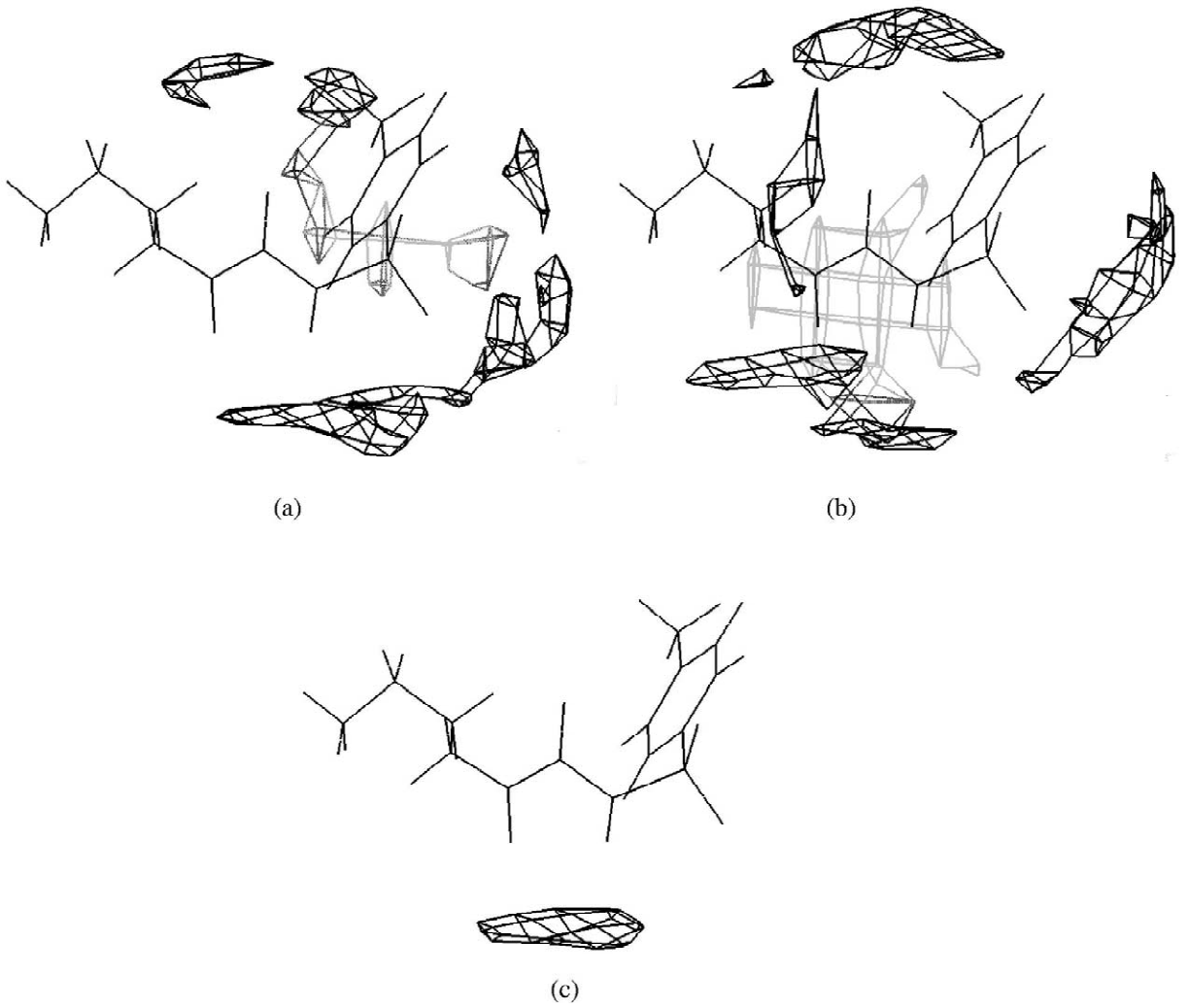

Fig. 6. The predicted preferential interaction sites of (a) water, (b) alkanes and (c) THF around tolbutamide.

counter to the proposed blocking mechanism but there is another equivalent preferential site lying close that was not targeted by the water. It is suggested that although the water can block access to one interaction site, its proximity to the second, unhindered, site may increase the interactions with probes at this site.

4. Conclusions

This paper has reviewed the use of molecular modelling techniques in the interpretation of inverse gas chromatography data. We have shown that the changes in the individual surface energetic parameters measured on materials that have been size reduced can be related to the increased exposure of the crystal plane with the smallest attachment energy and that the measured changes in surface energy mirror the exposure of particular chemical groups at that surface. In the examples where the surface energetic parameters were measure under different humidities, molecular modelling was used to identify the preferential interaction sites of the probes on a

host molecule. In the cases where interaction sites for water showed considerable differences to those for the probe molecules, no changes in the surface energetic parameters were measured. Where the preferential interaction sites for water corresponded with those for the probes, this was matched by a decrease in the measured interaction, suggesting that the water is blocking access to these sites. In the case of tolbutamide, the water only showed partial correspondence to the preferential site for THF and an increase was measured in the specific interaction with this probe. This suggested that the proximity of the water is activating this site. With these examples, it has been shown that the application of molecular modelling has given valuable insights into the interaction mechanisms underlying the measured changes.

References

[1] R. Docherty, in: A.S. Myerson, D.A. Green, P. Meenan (Eds.), ACS Conference Proceedings Series: Crystal Growth of Organic Materials, American Chemical Society, Washington, DC, 1996, p. 2.
[2] G. Clydesdale, K.J. Roberts, R. Docherty, J. Crystal Growth 135 (1994) 331.
[3] R.J. Roberts, R.C. Rowe, P. York, J. Mater. Sci. 29 (1994) 2289.
[4] P.J. Goodford, J. Med. Chem. 28 (1985) 849.
[5] P. York, M.D. Ticehurst, J.C. Osborn, R.J. Roberts, R.C. Rowe, Int. J. Pharm. 174 (1998) 179.
[6] L. Trowbridge, I.M. Grimsey, P. York, Pharm. Sci. (Suppl.) 1 (1998) 310.
[7] I.M. Grimsey, M.R. Sunkersett, J.C. Osborn, R.C. Rowe, P. York, Int. J. Pharm. 191 (1999) 43.
[8] M.R. Sunkersett, I.M. Grimsey, S.W. Doughty, J.C. Osborn, P. York, R.C. Rowe, in: Proceedings of the 20th Pharmaceutical Technology Conference, Liverpool, April 2001, 2001.
[9] M.R. Sunkersett, I.M. Grimsey, S.W. Doughty, J.C. Osborn, P. York, R.C. Rowe, Eur. J. Pharm. Sci. 13 (2001) 219.
[10] H. Balard, A. Saada, B. Siffert, E. Papirer, Clays Clay Minerals 45 (1997) 489.
[11] G.M. Dorris, D.G. Gray, J. Chem. Soc., Faraday Trans. 1 (77) (1981) 713.
[12] A.T. James, A.T.P. Martin, Biochem. J. 50 (1952) 679.
[13] J. Schultz, L. Lavielle, C. Martin, J. Adhesion 23 (1987) 45.
[14] M.W. Schmidt, K.K. Baldridge, J.A. Boatz, S.T. Elbert, M.S. Gordon, J.H. Jensen, S. Koseki, N. Matsunaga, K.A. Nguyen, S.J. Su, T.L. Windups, M. Dupuis, J.A. Montgomery, J. Comp. Chem. 14 (1993) 1347.
[15] C.M. Brakeman, K.B. Weber, J. Comp. Chem. 11 (1990) 361.
[16] S.L. Mayo, B.D. Larson, W.A. Goddard III, J. Phys. Chem. 94 (1990) 8897.
[17] D.H. Gay, A.L. Roil, J. Chem. Soc., Faraday Trans. 91 (1995) 925.